Recombination in compensated crystalline silicon for solar cells

Daniel Macdonald[a] and Andrés Cuevas
School of Engineering, College of Engineering and Computer Science, The Australian National University, Canberra, ACT 0200, Australia

(Received 8 November 2010; accepted 16 January 2011; published online 24 February 2011)

Deliberate compensation of crystalline silicon results in a decrease in the equilibrium carrier concentration, which leads to an increased carrier lifetime for the intrinsic recombination processes of Auger and radiative recombination. We present modeling which reveals that compensation also often leads to a significant increase in lifetime for recombination through defects via the Shockley–Read–Hall mechanism, a conclusion which is confirmed experimentally for the case of interstitial iron in *p*-type silicon. We show that the increased Shockley–Read–Hall lifetime can result from either an injection-level effect for deep levels, or from a Fermi-level effect for shallower levels. For cases where the defect exhibits no injection dependence of the carrier lifetime, compensation does not lead to an increased lifetime. Further modeling demonstrates that in certain cases, the lifetime increase can be expected to significantly outweigh the competing reductions in carrier mobilities and net doping, resulting in an improved short-circuit current, open-circuit voltage, and solar cell efficiency. © *2011 American Institute of Physics*.
[doi:10.1063/1.3555588]

I. INTRODUCTION

Low-cost solar-grade silicon materials often contain high concentrations of unwanted dopant species such as B, P, and Al.[1–3] Rather than undergoing expensive and energy-intensive purification steps to remove these dopants, an alternative is to add compensating dopants in order to achieve suitable resistivity values. Indeed, previous work has shown that such dopant compensation results in a significant improvement in the carrier lifetime,[4] courtesy of the reduced equilibrium carrier concentration. Accordingly, several research groups have demonstrated solar cell performance on compensated material that is comparable with noncompensated control cells.[5–8] In this work, we explore in more depth the underlying reasons for the improved carrier lifetimes in compensated silicon, both for intrinsic recombination processes such as Auger and radiative recombination, and also for recombination through defects, as governed by the Shockley–Read–Hall (SRH) model. We also demonstrate experimentally that it is indeed the net doping concentration, rather than the B and P concentrations themselves, that determines the recombination activity of recombination centers and, in particular, interstitial iron. Finally, we model the overall impact of compensation on solar cell parameters such as short-circuit current, open-circuit voltage, fill-factor, and efficiency, taking into account the competing effects of increased lifetimes and reduced net doping and carrier mobilities. The results suggest that for some practical SRH-limited cases, compensation can lead to improved device performance, although for certain cases compensation has no positive impact. For cases where compensation is beneficial, it can allow a greater tolerance of unintended dopants in solar-grade silicon feedstocks which might otherwise be too heavily doped for solar cell fabrication.

[a]Author to whom correspondence should be addressed. Electronic address: daniel.macdonald@anu.edu.au.

II. METHODS

Modeling the impact of compensation on the carrier lifetime and solar cell parameters (voltage, current, fill factor, and efficiency) was performed using the simulation program QSSMODEL.[9,10] This program allows the acceptor and donor concentrations N_A and N_D to be specified explicitly, enabling the impact of compensation on carrier mobilities to be determined using Klaassen's model.[11,12] It also allows simple extraction of the relevant data at a fixed generation rate, usually chosen as 0.1 suns in this work, unless otherwise stated (for example, for open-circuit voltage or short-circuit current determination the illumination is set to 1 sun, i.e., 100 mW/cm^2). A generation rate of 0.1 suns approximates the maximum power conditions in a working terrestrial solar cell. The modeling package also correctly accounts for nonuniform excess carrier profiles in the cell base when the minority carrier diffusion length becomes comparable to or less than the wafer thickness. The model is valid for low, intermediate, and high injection level conditions, and includes possible electric fields in the base region due to ohmic losses or to the mobility difference between electrons and holes. We have tested different mobility models, including that proposed by Arora *et al.*,[13] as used in the computer program PC1D,[14] and found that they have very little impact on the device output parameters (less than a 0.3% discrepancy in J_{sc}); therefore we have chosen to use Klaassen's model in low injection, since it accounts for small differences in electron and hole mobilities arising from whether the carriers are in the majority or minority. The low injection assumption is valid in the cases modeled here, since the excess carriers do not make an appreciable contribution to carrier scattering in comparison to lattice and ionized dopant scattering. The model automatically swaps from *p*-type to *n*-type silicon when $N_D > N_A$ by implementing straightforward changes to the carrier density and device voltage equations as well as to the direction of current flow.

 © 2011 American Institute of Physics

Author complimentary copy. Redistribution subject to AIP license or copyright, see http://jap.aip.org/jap/copyright.jsp

Within this model, intrinsic carrier lifetimes due to the combined impact of Auger and radiative recombination are determined using the empirical model of Kerr and Cuevas.[15] For calculating recombination lifetimes via the Shockley–Read–Hall model,[16,17] energy levels E_T and capture cross sections for electrons and holes σ_n and σ_p for two iron-related levels were $E_T = E_V + 0.38$ eV, $\sigma_n = 1.4 \times 10^{-14}$ cm^2, and $\sigma_p = 7 \times 10^{-17}$ cm^2 for interstitial Fe (Fe$_i$),[18,19] and $E_T = E_C - 0.26$ eV, $\sigma_n = 5 \times 10^{-15}$ cm^2, and $\sigma_p = 3 \times 10^{-15}$ cm^2 for the acceptor level for iron-boron pairs (FeB).[20] A third SRH level was also modeled, with assumed parameters of $E_T = E_C - 0.55$ eV, $\sigma_n = 10^{-16}$ cm^2, and $\sigma_p = 10^{-14}$ cm^2. These values are very similar to those of the acceptor level of substitutional gold[21] Au$_S$ ($E_T = E_C - 0.55$ eV, $\sigma_n = 1.4 \times 10^{-16}$ cm^2, and $\sigma_p = 7.6 \times 10^{-15}$ cm^2). However, in reality, the presence of the additional donor level for Au$_S$ makes the modeling more complex, since the dominant recombination level may be different in p- and n-type silicon, and so for the purposes of illustrating the principal effects, here we have modeled only the single acceptor level defined above. The thermal velocities v_{th} of electrons and holes were taken to be 1.1×10^7 cm/s.[22] For simulating solar cell performance, the front and rear surfaces were modeled with a saturation current density of $J_{0E} = 10^{-13}$ A cm^{-2} each, representative of standard modern solar cell technology. The AM1.5G spectrum and a temperature of 25 °C were assumed, together with a 75 nm thick silicon nitride antireflection coating on the front planar surface, and a wafer thickness 250 μm.

To demonstrate experimentally the impact of compensation on carrier lifetimes, compensated and noncompensated silicon wafers of various dopant concentrations were prepared with identical concentrations of interstitial iron, which is a strong and well characterized recombination center in silicon. The samples used were cleaved sections of p-type, ⟨100⟩-oriented Cz-Si wafers from three B-doped control ingots (noncompensated), and two compensated ingots, doped with both B and P, as described elsewhere.[23,24] The samples were etched, cleaned, and implanted with 70 keV Fe^{56} ions to a dose of 5×10^{10} cm^{-2} through a 30×30 mm^2 Si aperture. After further surface cleaning, the samples were annealed at 900 °C in nitrogen for 1 h, distributing the Fe uniformly throughout the sample thickness (140 μm), and resulting in a target volume Fe concentration of 3.6×10^{12} cm^{-3}. Note that this is below the solid solubility limit[18] of Fe at 900 °C, (approximately 4×10^{13} cm^{-3}), and hence precipitation is avoided. The low energy and dose used have previously been shown not to cause any significant residual lifetime-affecting damage after annealing.[25] The interstitial Fe concentration in a 1.2 Ω cm control sample was checked by measurement of the carrier lifetime before and after FeB pair dissociation,[26,27] and was found to be 3.4×10^{12} cm^{-3}, very close to the target value.

Plasma-enhanced chemical-vapor deposited SiN films were deposited on both surfaces at 400 °C for surface passivation. Effective carrier lifetimes were measured with the quasi-steady-state photoconductance technique.[28] This technique requires the sum of the electron and hole mobilities in order to calculate the carrier lifetime from the measured photoconductance. Klaassen's mobility model[11,12] was used to estimate the mobility sums in the compensated samples, using the acceptor and dopant concentrations N_A and N_D determined as described below.

The resistivities of the noncompensated control wafers were measured to be 0.50, 1.2, and 2.9 Ω cm, corresponding to boron concentrations N_A of 3.3×10^{16}, 1.3×10^{16}, and 5.3×10^{15} cm^{-3}, respectively. The resistivities of the compensated samples were 0.68 and 2.1 Ω cm, with B concentrations of 7.1×10^{16} and 4.0×10^{16} cm^{-3} respectively, determined via Fe-acceptor pairing measurements[23] as described elsewhere.[29] Using Klaassen's mobility model for majority carriers[11,12] (which has recently been shown to be accurate for majority carriers in compensated silicon[30]), combined with these resistivity and N_A values, and iterating until self-consistency is achieved, yields phosphorus concentrations N_D of 4.2×10^{16} and 3.2×10^{16} cm^{-3}, and net doping concentrations p_0 of 2.9×10^{16} and 8.5×10^{15} cm^{-3} respectively.

III. RESULTS AND DISCUSSION

A. Intrinsic recombination: Auger and radiative

Intrinsic recombination in crystalline silicon is comprised of Auger and radiative recombination. The carrier lifetime resulting from these intrinsic processes, $\tau_{intrinsic}$, is dependent on the equilibrium carrier concentrations n_0 and p_0, the excess carrier concentrations Δn and Δp, and the total carrier concentrations $n = n_0 + \Delta n$ and $p = p_0 + \Delta p$. In the absence of carrier trapping,[31] $\Delta n = \Delta p$. Kerr and Cuevas[15] developed a parameterization [their Eq. (24)] based on experimental results describing the combined impact of Auger and radiative recombination:

$$\tau_{intrinsic} = \frac{1}{(p_0 + n_0 + \Delta n)(1.8 \times 10^{-24} n_0^{0.65} + 6 \times 10^{-25} p_0^{0.65} + 3 \times 10^{-27} \Delta n^{0.8} + 9.5 \times 10^{-15})}, \quad (1)$$

where the final term in the denominator represents radiative processes, and the other three terms represent Auger processes. Clearly it is the net doping concentrations n_0 ($n_0 = N_D - N_A$ in n-type silicon) and p_0 ($p_0 = N_A - N_D$ in p-type silicon) that are the relevant parameters, rather than the dopant concentrations N_A and N_D themselves. As a consequence, the addition of compensating dopants, which reduce the net majority carrier concentration, can result in increased intrinsic lifetimes.

Figure 1 shows how the intrinsic lifetime, according to Eq. (1) above, varies as a function of the donor concentration N_D, for several fixed values of the acceptor concentration N_A. This is a useful way to present the results, since it

Author complimentary copy. Redistribution subject to AIP license or copyright, see http://jap.aip.org/jap/copyright.jsp

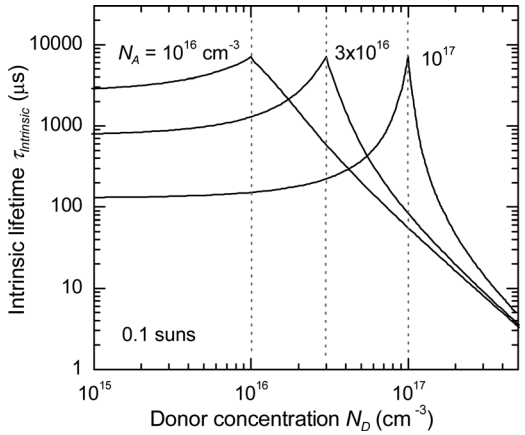

FIG. 1. The intrinsic lifetime $\tau_{\text{intrinsic}}$ due to Auger and radiative recombination in silicon as a function of the concentration of compensating donor atoms added N_D, under an illumination intensity of 0.1 suns. Three different acceptor concentrations N_A are shown, with the vertical dashed lines representing the intrinsic points where $N_A = N_D$.

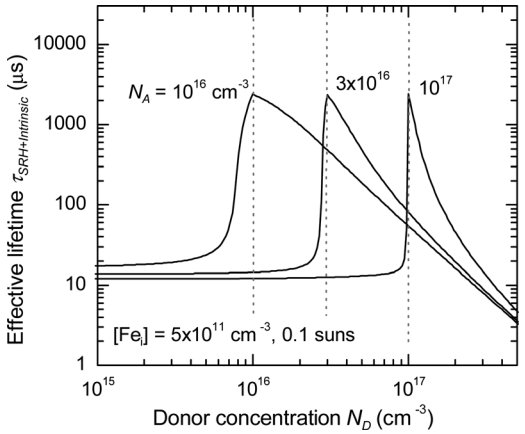

FIG. 2. The effective lifetime $\tau_{\text{SRH + intrinsic}}$ due to an interstitial iron concentration of $[\text{Fe}_i] = 5 \times 10^{11}$ cm^{-3}, and intrinsic recombination, as a function of the concentration of compensating donor atoms added N_D, under an illumination intensity of 0.1 suns, for three different acceptor concentrations N_A.

illustrates the effect of adding additional donor dopants to a material with a given amount of acceptors, as might be performed in practice. The lifetimes are calculated with a modeled illumination intensity of 0.1 "suns" (10 mW/cm^{-2} under the AM1.5G spectrum), which determines the excess carrier concentration Δn. This value was chosen as it represents approximately the maximum power point of a nonconcentrating solar cell. Note that for each curve there is an "intrinsic" point where $N_A = N_D$, shown as a vertical dotted line. To the left of the intrinsic point, the material is p-type, and to the right, n-type. The figure demonstrates the significant increase in intrinsic lifetime near the point of perfect compensation, due to the reduction in the free carrier concentrations ($n_0 = p_0 = n_i$). On the n-type side of the curves, the free electron concentration increases rapidly, and then becomes dominant, causing the intrinsic lifetimes to converge. It is possible to plot an equivalent figure for the case of fixed N_D values, as a function of added N_A, leading to n-type material on the left side, and p-type on the right, although for these intrinsic recombination processes, the result is qualitatively similar to Fig. 1.

B. Shockley–Read–Hall recombination

In reality, nonconcentrating silicon solar cells are rarely dominated by intrinsic recombination, but by recombination through defects and impurities. Such recombination can be represented with the SRH model, leading to a SRH lifetime τ_{SRH}:

$$\tau_{\text{SRH}} = \frac{\tau_{n0}(p_0 + p_1 + \Delta n) + \tau_{p0}(n_0 + n_1 + \Delta n)}{n_0 + p_0 + \Delta n}, \quad (2)$$

where τ_{n0} and τ_{p0} are the capture time constants for electrons and holes, related to the capture cross sections of the defect for electrons and holes σ_n and σ_p, the thermal velocity v_{th} and the recombination center concentration N via $\tau_{n0}^{-1} = N v_{\text{th}} \sigma_n$ and $\tau_{p0}^{-1} = N v_{\text{th}} \sigma_p$. The parameters n_1 and p_1 are, as usual, equal to the equilibrium electron and hole densities when the Fermi level is coincident with the recombination center energy level.

As with intrinsic recombination, the relevant doping parameters for determining the SRH lifetime are the net dopant concentrations n_0 and p_0, as opposed to the actual N_A and N_D values themselves. This allows the prospect of manipulating the SRH lifetime via compensation. Figure 2 shows the impact of compensation on the SRH lifetime, plotted in the same fashion as Fig. 1, but with the addition of 5×10^{11} cm^{-3} interstitial iron atoms (Fe$_i$) acting as SRH recombination centers. Note that the impact of intrinsic recombination is also included, and so the quantity plotted is actually the effective lifetime $1/\tau_{\text{eff}} = 1/\tau_{\text{SRH}} + 1/\tau_{\text{intrinsic}}$. The lifetimes are again calculated with a generation rate of 0.1 suns. The plot shows that the presence of the Fe$_i$ causes a large reduction in the lifetime compared to the intrinsic lifetimes in Fig. 1, when there is little compensation (i.e., at the very left hand side of the plot). However, as the concentration of donors is increased toward the intrinsic point, the reduction in the equilibrium carrier concentration p_0 causes both the SRH and intrinsic lifetimes to increase dramatically. This is the underlying physical reason for the improved carrier lifetimes in the more heavily compensated parts of silicon wafers recently observed by Dubois *et al.*[4]

While the curves in Fig. 2 reveal the global impact of compensation on SRH recombination, there are in fact two separate effects that can combine to yield an overall increase in the SRH lifetime. The first of these could be termed an "injection-level effect." This is depicted in Fig. 3, which shows the SRH lifetime for Fe$_i$ as a function of the excess carrier concentration Δn, for four different values of the net doping p_0. The case shown is for p-type silicon. Also shown on the plot is a diagonal line corresponding to a generation rate of 0.1 suns. The intersection between this diagonal line and the lifetime curves gives the corresponding lifetime near maximum power conditions. It can be seen that as p_0 decreases, the entire lifetime curve is shifted to the left, and the SRH lifetime at 0.1 suns increases. Such injection-level effects only occur for SRH centers that exhibit a strong injection dependence of the lifetime. Generally this occurs for deep levels with a much larger capture cross section for minority carriers than for majority carriers (as is the case for

Author complimentary copy. Redistribution subject to AIP license or copyright, see http://jap.aip.org/jap/copyright.jsp

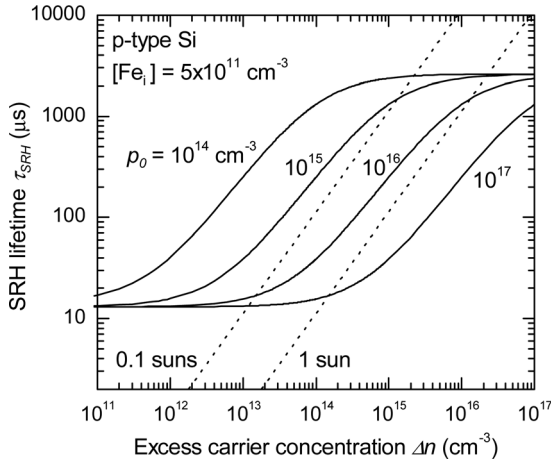

FIG. 3. The Shockley–Read–Hall (SRH) lifetime τ_{SRH} due to an interstitial iron concentration of $[Fe_i] = 5 \times 10^{11}$ cm^{-3} as a function of the excess carrier density Δn, for four different values of the net doping p_0. The dashed lines represent generation rates of 0.1 suns (near maximum power conditions) and 1 sun (open-circuit conditions).

Fe$_i$ in *p*-type silicon). Note that, by contrast, in *n*-type silicon, Fe$_i$ exhibits no injection dependence,[32] and therefore compensation would not result in an increase of the carrier lifetime (although the impact on the lifetime per Fe atom is much reduced in *n*-type silicon anyway).

The second effect could be referred to as a "Fermi-level effect" and applies to shallower levels that are positioned near the Fermi level, or its mirror image in the opposite band-half. An example is shown in Fig. 4 for the case of the acceptor level of FeB pairs. Again, the figure clearly shows that a decrease in the net doping p_0 results in an increase in the lifetime at 0.1 suns. However, this is caused predominantly by a change in the shape of the lifetime curve, rather than a simple horizontal shift (although the horizontal shift caused by the injection-level effect is also present). Such a change in shape occurs when either p_1 or n_1 becomes comparable to p_0 or n_0 in the SRH expression, or in other words, when the Fermi level is near the defect level (or its mirror image in the other band-half). For net doping concentrations typical of solar cells, this means that such levels must be relatively shallow (less than approximately 0.2 eV from either band edge for a net doping of 10^{16} cm^{-3}). In general, it is the deeper levels like Fe$_i$ that are most detrimental in silicon solar cells, and so the injection-level effect is likely to be more important in practice than the Fermi-level effect.

With this distinction in mind, it is clear that the injection level effect plays a large role in Fig. 2 for Fe$_i$. The larger capture cross section for electrons results in a strong injection dependence in *p*-type silicon, causing the dramatic increase in lifetime as the degree of compensation is increased on the *p*-type side of the intrinsic points in Fig. 2. In contrast, on the *n*-type side of the intrinsic points, the presence of Fe$_i$ has a much lower impact on the lifetime, and the curves follow the intrinsic lifetimes of Fig. 1 quite closely.

In contrast to the donor level for Fe$_i$, deep acceptor levels in silicon, such as occur for Au$_S$ or Zn$_S$,[21] often have a reversed capture cross section asymmetry.[33] This means that they have a much greater recombination activity in *n*-type silicon, with strong injection dependence, while in *p*-type silicon they have little impact and no injection-dependence. Therefore, compensation does not result in an increase in the SRH lifetime in *p*-type silicon for such levels, although it has a dramatic effect in *n*-type silicon. This can be seen in Fig. 5, which shows the combined effect of an acceptor level at $E_C - 0.55$ eV and a large capture cross section asymmetry, and intrinsic recombination, for a generation rate of 0.1 suns, in analogy with Fig. 2 for Fe$_i$. On the *p*-type side there is only a small positive impact of compensation, which is caused entirely by the intrinsic processes as shown in Fig. 1. On the *n*-type side, however, near the intrinsic point there is a strong positive effect from increasing compensation (i.e., moving from the right hand side of the plot toward the intrinsic point).

These examples serve to show that for the case of SRH recombination, compensation can have a beneficial impact on the carrier lifetime, just as it can for intrinsic recombination processes. However, for SRH recombination, the magnitude of the impact depends very sensitively on the energy

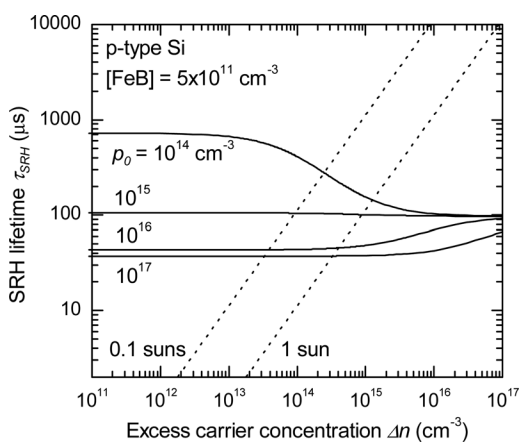

FIG. 4. The Shockley–Read–Hall (SRH) lifetime τ_{SRH} due to an iron-boron pair concentration of $[FeB] = 5 \times 10^{11}$ cm^{-3} as a function of the excess carrier density Δn, for four different values of the net doping p_0. The dashed lines represent generation rates of 0.1 suns (near maximum power conditions) and 1 sun (open-circuit conditions).

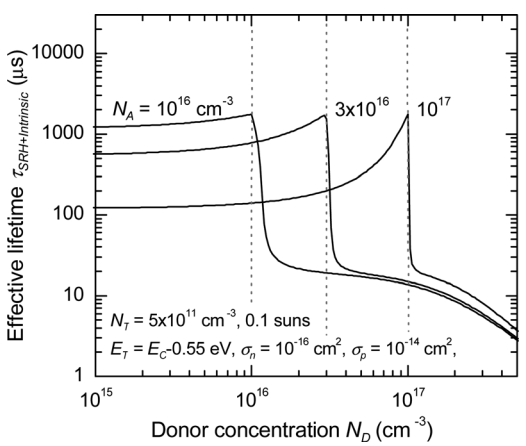

FIG. 5. The effective lifetime $\tau_{SRH+intrinsic}$ due to an acceptor SRH center with a concentration of $N_T = 5 \times 10^{11}$ cm^{-3}, and intrinsic recombination, as a function of the concentration of compensating donor atoms added N_D, under an illumination intensity of 0.1 suns, for three different acceptor concentrations N_A.

Author complimentary copy. Redistribution subject to AIP license or copyright, see http://jap.aip.org/jap/copyright.jsp

levels and capture cross sections of the defect in question. Since many of the common metallic impurities in silicon,[32] as well as the well-known boron-oxygen defect,[34,35] tend to exhibit a strong injection dependence of the carrier lifetime in *p*-type silicon, it is likely that compensation will be of greater benefit in *p*-type materials.

To demonstrate experimentally that it is indeed the net doping, rather than the dopant concentrations, which determines the SRH lifetime, we measured carrier lifetimes on Cz wafers containing identical doses of interstitial Fe, prepared and measured as described above. Immediately prior to measurement, the samples were subject to strong light pulses to break any FeB pairs and ensure that the majority of the Fe was in the isolated interstitial state, which should provide a strong distinction between different values of p_0 due to the injection-level effect described above (this is in contrast to FeB pairs, which have little injection-dependence over the doping range available). The lifetimes were measured at an excess carrier density of 1×10^{15} cm^{-3}, and the results are shown in Fig. 6. For the control samples, which were noncompensated, and for which $N_A = p_0$, the lifetimes decrease steadily as a function of p_0, as expected from Fig. 3. The two compensated samples are also plotted in Fig. 6. When plotted as a function of p_0, they align very well with the control samples, whereas if plotted as a function of N_A, they lie well away from the expected trend. This serves to show conclusively that it is indeed the net doping which determines the SRH lifetime in compensated silicon, in support of the modeling results described above.

C. Impact on device voltage

The previous section demonstrated that the presence of compensation can significantly improve the carrier lifetime in silicon dominated either by intrinsic or SRH recombination. However, the carrier lifetime is only one of several critical parameters that determine the efficiency of a solar cell. Other important electrical properties are the net doping concentration p_0 or n_0, which, together with the lifetime, determine the device voltage; and the carrier mobilities, which affect the resistivity (majority carrier mobility) and short circuit current (minority carrier mobility).

For a *p*-type base, the voltage of a front-junction n^+pp^+ device is given by

$$V = \frac{kT}{q} \ln\left(\frac{(n_0 + \Delta n_{\text{front}})(p_0 + \Delta n_{\text{back}})}{n_i^2}\right) + V_{\text{base}}, \quad (3)$$

where Δn_{front} and Δn_{back} are the excess carrier densities at the edges of the space-charge regions of the front n^+p junction and the rear pp^+ high-low junction respectively, n_i is the intrinsic carrier concentration, and V_{base} is the electrostatic drop across the base region due to ohmic losses and to the difference between electron and hole mobilities.

In steady-state, the average excess carrier concentration is directly related to the effective carrier lifetime via $\Delta n_{\text{av}} = G\tau_{\text{eff}}$, where G is the average carrier generation rate. Compensation acts to reduce the net doping p_0, but, as shown above, also to increase the lifetime τ and therefore the excess carrier density Δn. Clearly it is important to determine which of these competing effects is dominant, in order to assess the potential of compensation to improve device voltages.

Figure 7 shows the open-circuit voltage for a solar cell with $[\text{Fe}_i] = 5 \times 10^{11}$ cm^{-3}, with intrinsic recombination included, and for three different acceptor concentrations N_A, as a function of the added donor concentration N_D. The figure shows that, for the cases with $N_A = 10^{16}$ and 3×10^{16} cm^{-3}, the voltage does indeed increase monotonically with compensation on the *p*-type side of the intrinsic point, demonstrating that the improvement in lifetime caused by compensation outweighs the reduction in the net doping p_0. For the curve with $N_A = 10^{17}$ cm^{-3}, however, there is an initial decrease in voltage with increasing compensation, until very strong compensation is reached, when a rapid increase in voltage occurs. This initial decrease is caused by the fact that under 1 sun, the carrier lifetime is near the injection-independent region, as also shown for the $p_0 = 10^{17}$ cm^{-3} case in Fig. 3. The lifetime therefore does not increase strongly with

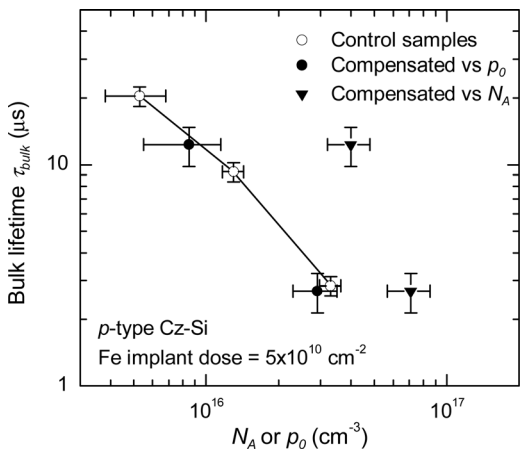

FIG. 6. Measured bulk carrier lifetimes at an excess carrier density of $\Delta n = 10^{15}$ cm^{-3}, for *p*-type silicon wafers containing the same concentration of interstitial iron, as a function of either the total acceptor concentration N_A, or the net doping $p_0 = N_A - N_D$. Three noncompensated control samples are plotted as a function of N_A, while the two compensated samples are plotted both as a function of N_A and p_0. The solid line is a guide to the eye for the control samples.

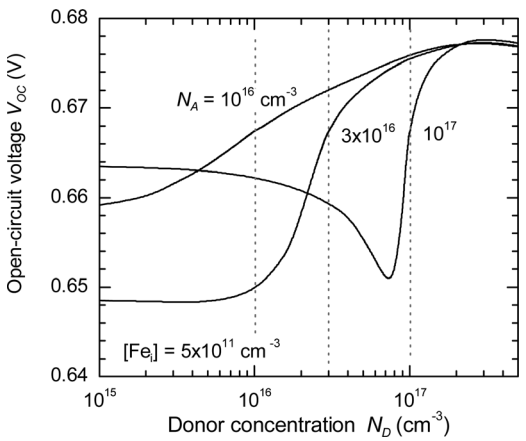

FIG. 7. The open-circuit voltage V_{OC}, with intrinsic recombination and an interstitial iron concentration of $[\text{Fe}_i] = 5 \times 10^{11}$ cm^{-3}, as a function of the concentration of compensating donor atoms added N_D, for three different acceptor concentrations N_A.

Author complimentary copy. Redistribution subject to AIP license or copyright, see http://jap.aip.org/jap/copyright.jsp

compensation, and the simultaneous reduction in p_0 causes a drop in the voltage. At very high compensation, the injection-level effect begins to dramatically increase the 1 sun lifetime, leading to a significant increase in voltage.

Note, however, that these results are not general. For example, for interstitial Fe in *n*-type silicon, in which there is no injection-dependence of the carrier lifetime for any net doping level, increased compensation does not improve the lifetime, but does lower the net doping n_0, leading to a drop in V_{OC}, as seen on the *n*-type side of the intrinsic point in Fig. 7. Essentially then, for compensation to result in a net improvement in V_{OC}, the carrier lifetime has to be strongly injection dependent under the illumination intensity of interest, either through the injection-level or Fermi-level effects described above, in order to overcome the simultaneous reduction in the net doping.

D. Impact on device current

Compensation is also known to cause a decrease in the carrier mobilities μ, due to the presence of additional ionized dopant scattering centers.[30,36,37] The current collected at the *p-n* junction in a solar cell increases monotonically with the minority carrier diffusion length $L_D = (D\tau)^{0.5}$, where D is the minority carrier diffusivity and is related to the mobility via $D = \mu kT/q$. Consequently, there are again competing affects of compensation on device current—increased lifetimes act to increase the minority carrier diffusion length but reduced mobilities have the opposite effect. Taking both of these effects into account, Fig. 8 shows the evolution of the short circuit current with increasing compensation, for the same cases described in Sec. III C above. Here we have used Klaassen's model for the minority carrier mobilities. Recent experimental results[30] have indicated that this model may somewhat overestimate minority carrier mobilities in compensated silicon; however, in the absence of a proven alternative, we have used it here to demonstrate the key principles.

Figure 8 shows that that the net impact of compensation on the short-circuit current on the *p*-type side of the intrinsic point is positive for all three N_A values, in contrast to the V_{OC} curves described above. This indicates that the reduced mobilities are always outweighed by the increased carrier lifetime. At first it might seem surprising that the effective carrier lifetime is improved by compensation under short-circuit conditions, since the excess carrier density in the base is expected to be low, perhaps low enough to avoid the injection dependence of the carrier lifetime. However, the modeling shows that the average excess carrier density under short circuit condition is actually only slightly lower than at maximum power (typically about half). Therefore, a generation rate of 0.1 suns, as shown in Figs. 3 and 4, is also quite close to short-circuit conditions, revealing that compensation can indeed cause a significant improvement in carrier lifetime under short-circuit. Note that, in general, the square root dependence of the J_{SC} on the carrier lifetime, as opposed to the logarithmic dependence for the V_{OC}, makes the J_{SC} more sensitive to increases in the lifetime. This is compounded by the much weaker dependence of the mobilities on the dopant concentrations N_A and N_D, compared to the net doping. Note, however, that for solar cells with minority carrier diffusion lengths longer than the base thickness, the dependence of the J_{SC} on the diffusion length is weaker than the square root dependence for a "long base" device, and the benefits of compensation on the J_{SC} will be diminished. Nevertheless, in many practical cases it is true that the impact of compensation is expected to be more positive for the cell current than the voltage.

E. Impact on fill factor

The fill factor of the photovoltaic *I-V* curve was also modeled for the cases described above, and is shown in Fig. 9. The significant drop in fill factor for all three curves with increasing compensation on the *p*-type side is predominantly caused by the strongly injection-dependent carrier lifetime of Fe_i in *p*-type silicon, an effect which has been documented previously in noncompensated devices.[38] It is essentially caused by the fact that the lifetime at maximum power is significantly lower than at open-circuit. As the compensation becomes stronger, the lifetime at the maximum power point moves toward higher injection levels, reducing

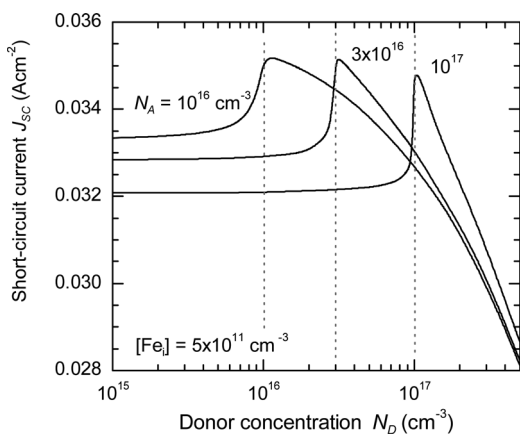

FIG. 8. The short-circuit current J_{SC}, with intrinsic recombination and an interstitial iron concentration of $[Fe_i] = 5 \times 10^{11}$ cm^{-3}, as a function of the concentration of compensating donor atoms added N_D, for three different acceptor concentrations N_A.

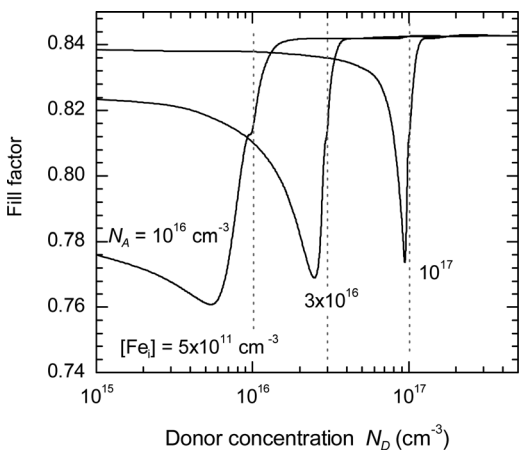

FIG. 9. The fill factor, with intrinsic recombination and an interstitial iron concentration of $[Fe_i] = 5 \times 10^{11}$ cm^{-3}, as a function of the concentration of compensating donor atoms added N_D, for three different acceptor concentrations N_A.

Author complimentary copy. Redistribution subject to AIP license or copyright, see http://jap.aip.org/jap/copyright.jsp

the difference with open-circuit conditions, and leading to a recovery of the fill factor.

The modeling also accounts for the increased resistive losses in the base caused by the reduced net doping. This causes a reduction in the fill factor down to a value of approximately 0.81 near the intrinsic point, which is visible in Fig. 9 as a small kink in the curves. Note that the effect of the increased resistivity of the base is greatly mitigated by the presence of light-generated carriers through the well known mechanism of conductivity modulation.

It should be noted that the fill factor values in Fig. 9 represent upper limits of what could be achieved in real solar cells, since they do not account for resistive losses associated with the metallization or lateral transport in the emitter.

F. Impact on device efficiency

Figure 10 shows the modeled solar cell efficiencies for the cases discussed above. For all three N_A values there is an initial drop in efficiency, followed by a significant improvement close to the intrinsic point. For the $N_A = 10^{16}$ and 3×10^{16} cm^{-3} cases, the initial drop is caused by the reduction in the fill factor associated with the injection-dependent lifetimes, while for the $N_A = 10^{17}$ cm^{-3} case, this effect is further compounded by the drop in V_{OC}. The results show that compensation can, in principle, lead to an improvement in solar cell efficiency, provided that the compensation is sufficiently strong. However, as mentioned above, this is not generally true, and depends on the properties of the dominant recombination centers. In cases where there is no injection-level dependence of the carrier lifetime, for example, Fe_i in n-type silicon, the V_{OC}, J_{SC}, and efficiency would all decrease with increasing compensation. This is evident on the n-type side of the plots in Fig. 10, which show a reduction in efficiency very close to the intrinsic point, as it is approached from the right hand side.

As noted above, the range of donor concentrations for which the efficiency is significantly improved is quite small on the p-type side of the intrinsic point. In other words, compensation has to be quite strong (i.e., $N_D > 0.5\ N_A$ even for the most favorable case in Fig. 10 with $N_A = 10^{16}$ cm^{-3}) for a noticeable effect. This requirement obviously creates challenges in terms of dopant segregation during ingot growth. However, possible solutions to this problem, for example using gallium codoping in order to generate uniform resistivity profiles, have been proposed.[39–41] For completeness, Fig. 11 shows the resistivity curves computed using Klaassen's mobility model for the cases modeled above.

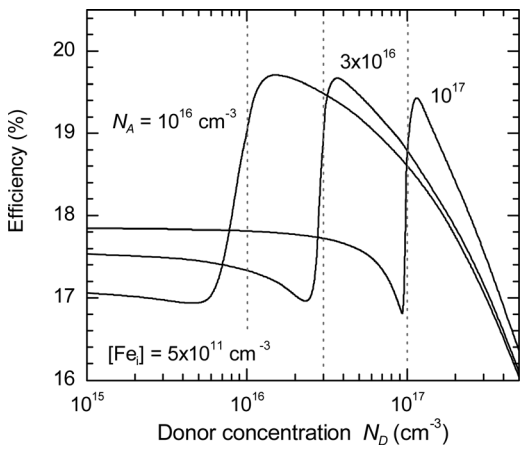

FIG. 10. The solar cell efficiency, with intrinsic recombination and an interstitial iron concentration of $[Fe_i] = 5 \times 10^{11}$ cm^{-3}, as a function of the concentration of compensating donor atoms added N_D, for three different acceptor concentrations N_A.

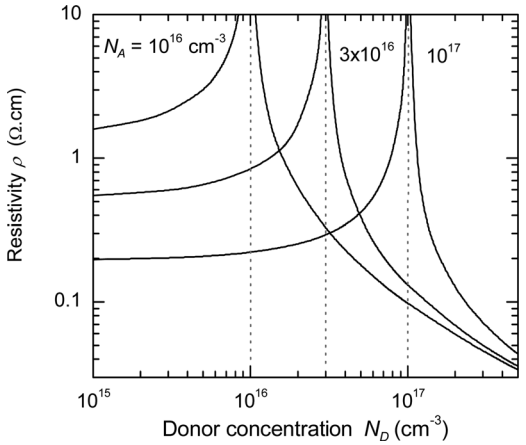

FIG. 11. The resistivity ρ as a function of the concentration of compensating donor atoms added N_D, for three different acceptor concentrations N_A.

Finally, it is worth noting that, ultimately, the discussion above largely reflects the usual trade-offs in finding the optimal base resistivity for solar cells.[42] Indeed, in terms of recombination, the case of an uncompensated cell with $N_A = 10^{16}$ cm^{-3} is entirely identical to a compensated device with $N_A = 5 \times 10^{16}$ cm^{-3}, $N_D = 4 \times 10^{16}$ cm^{-3}, and $p_0 = 10^{16}$ cm^{-3}. The only differences that can arise are due to the reduced mobilities, which may affect the cell current or, importantly, if additional defects are created whose concentrations are determined by the chemical presence of one of the dopant species. A key dopant-related recombination center is the well-known boron-oxygen related defect.[43] However, it has recently been shown that its concentration in p-type silicon is in fact determined by the net doping,[24] rather than the boron concentration, and so even for this defect, a compensated base should behave precisely as a noncompensated base with the same net doping, at least in terms of recombination.

IV. CONCLUSIONS

Experimental and modeling results confirm that dopant compensation can lead to a significant increase in the carrier lifetime in silicon wafers, for both intrinsic processes such as Auger and radiative recombination, and also for recombination through defects (SRH). In the case of SRH recombination, the increase occurs due to the injection dependence of the carrier lifetime, which can be caused either by an injection-level effect for deep centers, or a Fermi-level effect for shallower centers. In cases where there is no injection dependence of the carrier lifetime, such as interstitial iron in n-type silicon, compensation does not lead to an improved carrier lifetime. Modeling has also demonstrated that the improved lifetimes caused by compensation can translate

Author complimentary copy. Redistribution subject to AIP license or copyright, see http://jap.aip.org/jap/copyright.jsp

into higher open-circuit voltages, short-circuit currents, and cell efficiencies, under certain conditions. A positive impact on device current occurs when the increase in lifetime outweighs the simultaneous reduction in carrier mobility, which is achieved quite easily, while the device voltage improves when the lifetime increases more rapidly than the counterbalancing reduction in the net doping. The fill factor is usually reduced by a combination of injection-dependent lifetimes and, to a lesser degree, by increased ohmic losses in the base. In general, for an overall improvement in solar cell conversion efficiency, the degree of compensation has to be strong. Nevertheless, the results demonstrate that, in principle, deliberate compensation of low-cost solar-grade silicon materials, which would otherwise have very low resistivities, can allow reasonable device performance to be achieved without expensive additional purification steps.

ACKNOWLEDGMENTS

D.M. was supported by an Australian Research Council QEII Fellowship. The authors are grateful to Kai Petter of Q-cells and Bart Geerligs of ECN for kindly providing the compensated silicon wafers, AnYao Liu of ANU for assisting with measurements, Chris Samundsett of ANU for assisting with sample preparation, and Professor Rob Elliman of ANU for access to the ion implantation equipment.

[1]N. Yuge, M. Abe, K. Hanazawa, H. Baba, N. Nakamura, Y. Kato, Y. Sakaguchi, S. Hiwasa, and F. Aratani, Prog. Photovoltaics **9**, 203 (2001).
[2]D. Sarti and R. Einhaus, Sol. Energy Mater. Sol. Cells **72**, 27 (2002).
[3]J. Degoulange, I. Perichaud, C. Trassy and S. Martinuzzi, Sol. Energy Mater. Sol. Cells **92**, 1269 (2008).
[4]S. Dubois, N. Enjalbert, and J. P. Garandet, Appl. Phys. Lett. **93**, 032114 (2008).
[5]J. Libal, S. Novaglia, M. Acciarri, S. Binetti, R. Petres, J. Arumughan, R. Kopecek, and A. Prokopenko, J. Appl. Phys. **104**, 104507 (2008).
[6]A. Halm, J. Jourdan, S. Nichol, B. Ryningen, H. Tathgar, and R. Kopecek, in *Proceedings 35th IEEE Photovoltaics Specialists Conference,* Honolulu, Hawaii (IEEE, New York, 2010), pp. 1023–1027 .
[7]C. Modanese, M. D. Sabatino, A.-K. Søiland, K. Peter, and L. Arnberg, Prog. Photovoltaics: Res. Appl. **19**, 45–53 (2011).
[8]S. Rein, J. Geilker, W. Kwapil, G. Emanuel, I. Reis, A. K. Soiland, S. Grandum, and R. Tronstad, in *Proceedings 25th European Photovoltaic Solar Energy Conference,* Valencia, Spain (WIP Renewable Energies, Munich, 2010), pp. 1186–1194.
[9]A. Cuevas and R. Sinton, in *22nd European Photovoltaics Solar Energy Conference*, Milan, Italy (WIP-Renewable Energies, Munich, 2007), p. 38.
[10]A. Cuevas and R. A. Sinton, in *Proceedings 23rd European Photovoltaic Solar Energy Conference*, Valencia, Spain (WIP-Renewable Energies, Munich, 2008), p. 315.
[11]D. B. M. Klaassen, Solid-State Electron. **35**, 953 (1992).
[12]D. B. M. Klaassen, Solid-State Electron. **35**, 961 (1992).
[13]N. D. Arora, J. R. Hauser, and D. J. Roulston, IEEE Trans. Electron Devices **29**, 292 (1982).
[14]P. A. Basore and D. A. Clugston, *PC1D V5.3* (University of New South Wales, Sydney, 1998).
[15]M. J. Kerr and A. Cuevas, J. Appl. Phys. **91**, 2473 (2002).
[16]R. N. Hall, Phys. Rev. **87**, 387 (1952).
[17]W. Shockley and W. T. Read, Phys. Rev. **87**, 835 (1952).
[18]A. A. Istratov, H. Hieslmair, and E. R. Weber, Appl. Phys. A **69**, 13 (1999).
[19]D. Macdonald, J. Tan and T. Trupke, J. Appl. Phys. **103**, 073710 (2008).
[20]D. Macdonald, T. Roth, P. N. K. Deenapanray, T. Trupke, and R. A. Bardos, Appl. Phys. Lett. **89**, 142107 (2006).
[21]K. Graff, *Metal Impurities in Silicon-Device Fabrication,* Springer Series in Material Science Vol. 24 (Springer-Verlag, Berlin, 2000).
[22]W. M. Bullis and H. R. Huff, J. Electrochem. Soc. **143**, 1399 (1996).
[23]D. Macdonald, A. Cuevas, and L. J. Geerligs, Appl. Phys. Lett. **92**, 202119 (2008).
[24]D. Macdonald, F. Rougieux, A. Cuevas, B. Lim, J. Schmidt, M. DiSabatino, and L. J. Geerligs, J. Appl. Phys. **105**, 093704 (2009).
[25]D. Macdonald, P. N. K. Deenapanray, and S. Diez, J. Appl. Phys. **96**, 3687 (2004).
[26]G. Zoth and W. Bergholz, J. Appl. Phys. **67**, 6764 (1990).
[27]D. Macdonald, L. J. Geerligs, and A. Azzizi, J. Appl. Phys. **95**, 1021 (2004).
[28]R. A. Sinton and A. Cuevas, Appl. Phys. Lett. **69**, 2510 (1996).
[29]D. Macdonald and A. Liu, Phys. Status Solidi B **247**, 2218 (2010).
[30]F. E. Rougieux, D. Macdonald, A. Cuevas, S. Ruffell, J. Schmidt, B. Lim, and A. Knights, J. Appl. Phys. **108**, 013706 (2010).
[31]D. Macdonald and A. Cuevas, Phys. Rev. B **67**, 075203 (2003).
[32]D. Macdonald and L. J. Geerligs, Appl. Phys. Lett. **85**, 4061 (2004).
[33]C. T. Sah, P. Chan, C. K. Wang, R. L. Y. Sah, K. A. Yamakawa, and R. Lutwack, IEEE Trans. Electron Devices **28**, 304 (1981).
[34]S. Rein and S. W. Glunz, Appl. Phys. Lett. **82**, 1054 (2003).
[35]K. Bothe, R. Sinton, and J. Schmidt, Prog. Photovoltaics **13**, 287 (2005).
[36]S. Pizzini and C. Calligarich, J. Electrochem. Soc. **131**, 2128 (1984).
[37]J. Veirman, S. Dubois, N. Enjalbert, J. P. Garandet, D. R. Heslinga, and M. Lemiti, Solid-State Electron. **54**, 671 (2010).
[38]D. Macdonald and A. Cuevas, Prog. Photovoltaics **8**, 363 (2000).
[39]C. Bucher, D. L. Meier, D. Leblanc, and R. Boisvert, International patent WO 2008/112598 A2 (2008).
[40]J. Kraiem, R. Einhaus and H. Lauvray, in *Proceedings 34th IEEE Photovoltaic Specialists Conference,* Philadelphia (IEEE, New York, 2009), p. 1327.
[41]M. Forster, E. Fourmond, R. Einhaus, H. Lauvray, J. Kraiem, and M. Lemiti, in *Proceedings 25th European Photovoltaic Solar Energy Conference,* Valencia, Spain (WIP-Renewable Energies, Munich, in press).
[42]L. J. Geerligs and D. Macdonald, Prog. Photovoltaics **12**, 309 (2004).
[43]J. Schmidt and K. Bothe, Phys. Rev. B **69**, 024107 (2004).

Author complimentary copy. Redistribution subject to AIP license or copyright, see http://jap.aip.org/jap/copyright.jsp